

# Hierarchy independent sensitivity to leptonic $\delta_{CP}$ with atmospheric neutrinos

D. Indumathi,<sup>1,2,\*</sup> S. M. Lakshmi,<sup>3,†</sup> and M. V. N. Murthy<sup>1,‡</sup>

<sup>1</sup>*The Institute of Mathematical Sciences, Chennai 600 113, India*

<sup>2</sup>*Homi Bhabha National Institute, Training School Complex,  
Anushakti Nagar, Mumbai 400085, India*

<sup>3</sup>*Indian Institute of Technology Madras, Chennai 600 036, India*

(Dated: March 6, 2024)

## Abstract

The Dirac leptonic CP phase  $\delta_{CP}$  is one of the crucial unknown parameters in neutrino oscillation physics. In this paper we explore the possibility of using low energy atmospheric neutrino events to probe  $\delta_{CP}$ . We show that at sub GeV energies, when the events are binned as a function of the energy and direction of the final state leptons, a consistent distinction between various true  $\delta_{CP}$  values is obtained. We also show that at these energies there is no sensitivity to the mass ordering/hierarchy, so that  $\delta_{CP}$  can be measured without hierarchy ambiguity. In addition a preliminary  $\chi^2$  analysis of the sensitivity to  $\delta_{CP}$  using atmospheric neutrinos assuming a generic detector with perfect separation between charged current  $\nu_\mu, \bar{\nu}_\mu, \nu_e$  and  $\bar{\nu}_e$  events is given.

---

\*Electronic address: indu@imsc.res.in

†Electronic address: slakshmi@physics.iitm.ac.in

‡Electronic address: murthy@imsc.res.in

## I. INTRODUCTION

The Dirac leptonic phase  $\delta_{CP}$  is one of the important unknown parameters in neutrino oscillation physics today. Although there is a hint that its value is approximately  $\delta_{CP} \approx -145^\circ$  ( $-76^\circ$ ) for normal (inverted) hierarchy [1], several experiments, mainly accelerator long base line (LBL) experiments are running/are being designed to measure this parameter precisely [2–4]. These accelerator LBL experiments will have very high sensitivity to  $\delta_{CP}$  (especially DUNE) on their own; however, it is important to study the sensitivity from atmospheric neutrinos also. Several atmospheric neutrino experiments are currently running [5–7] and are proposed [8–13] to probe different neutrino oscillation parameters. Although these experiments have smaller fluxes compared to the accelerator LBL ones, they probe a wide range of neutrino baselines and energies,  $L_\nu$  and  $E_\nu$ , and hence can be used to probe a wide variety of physics scenarios. Also atmospheric neutrino fluxes peak at sub GeV energies [14–16]; and atmospheric neutrino experiments do not require separate runs for  $\nu$  and  $\bar{\nu}$  unlike the accelerator LBL experiments.

In this paper, we explore the possibility of using atmospheric neutrino events, especially those in the sub GeV region ( $E_\nu < 1$  GeV) to probe the CP phase  $\delta_{CP}$ . It has been shown earlier [17–20] that atmospheric neutrinos at energies above a GeV or so are completely *insensitive* to the CP phase and hence can be used to measure the neutrino mass ordering/hierarchy (MH) *independent* of the CP phase. This is in contrast to beam experiments where degeneracies give rise to ambiguities in the extraction of these oscillation parameters so that the MH determination is entangled with and depends on the true value of  $\delta_{CP}$ .

In this paper, we show for the first time that both the  $\nu_e$  and  $\nu_\mu$  atmospheric neutrino events at low, i.e., sub-GeV, energies are sensitive to the CP phase. In addition, the dependence on the CP phase (of the angular distribution) of  $\nu_e$  and  $\nu_\mu$  events is such that it *systematically* shifts the observed event rates in *opposite* directions in the two cases. Finally, this dependence on CP is *independent* of the mass hierarchy. Thus we propose that a measurement of sub-GeV atmospheric neutrino events, where event rates are large, will be able to determine  $\delta_{CP}$  cleanly, independent of the mass hierarchy (MH). That is, atmospheric neutrino events are uniquely positioned so that *low energy sub-GeV events are sensitive to  $\delta_{CP}$  independent of MH*, while *higher energy (few GeV) events are sensitive to MH independent of  $\delta_{CP}$* . We believe that this unique dependence has been discussed for the first time, in this paper.

In particular, we show in Section II that the events spectra for different values of the true  $\delta_{CP}$  are different when the events are binned as a function of the energy and direction of the final state lepton in the charged current (CC) interaction, thus making it possible to have a good  $\delta_{CP}$  sensitivity. In Section. III we show analytically, that at such low energies and larger baselines which are relevant for atmospheric neutrinos,  $\delta_{CP}$  can be determined *irrespective of hierarchy*. We quantify our results in Section. IV with a preliminary and simple  $\chi^2$  analysis of the events that would be obtained with a detector with perfect resolutions and efficiencies, and ignoring systematic effects. We end with discussions and conclusions which are presented in Section. V.

## II. OSCILLATION PROBABILITIES AND ATMOSPHERIC NEUTRINO EVENTS AT SUB GEV ENERGIES

In the case of atmospheric neutrinos, the muon neutrino (and anti-neutrino) fluxes  $\Phi_\mu + \bar{\Phi}_\mu$  are larger than that of the electron neutrino (and anti-neutrino) fluxes  $\Phi_e + \bar{\Phi}_e$ . The sensitivity to  $\delta_{CP}$  in these events arises from the transition probabilities  $P_{\mu e}, \bar{P}_{\mu e}$  and  $P_{e\mu}, \bar{P}_{e\mu}$  [21–23]. Hence the sensitivity to  $\delta_{CP}$  will be larger for electron like events as compared to the muon like events. A comparison of the relevant oscillation probabilities for two different values of  $\delta_{CP}$  as a function of  $\cos \theta_\nu$  (neutrino direction) for a sample sub-GeV neutrino energy,  $E_\nu = 0.65$  GeV is shown in Fig. 1.

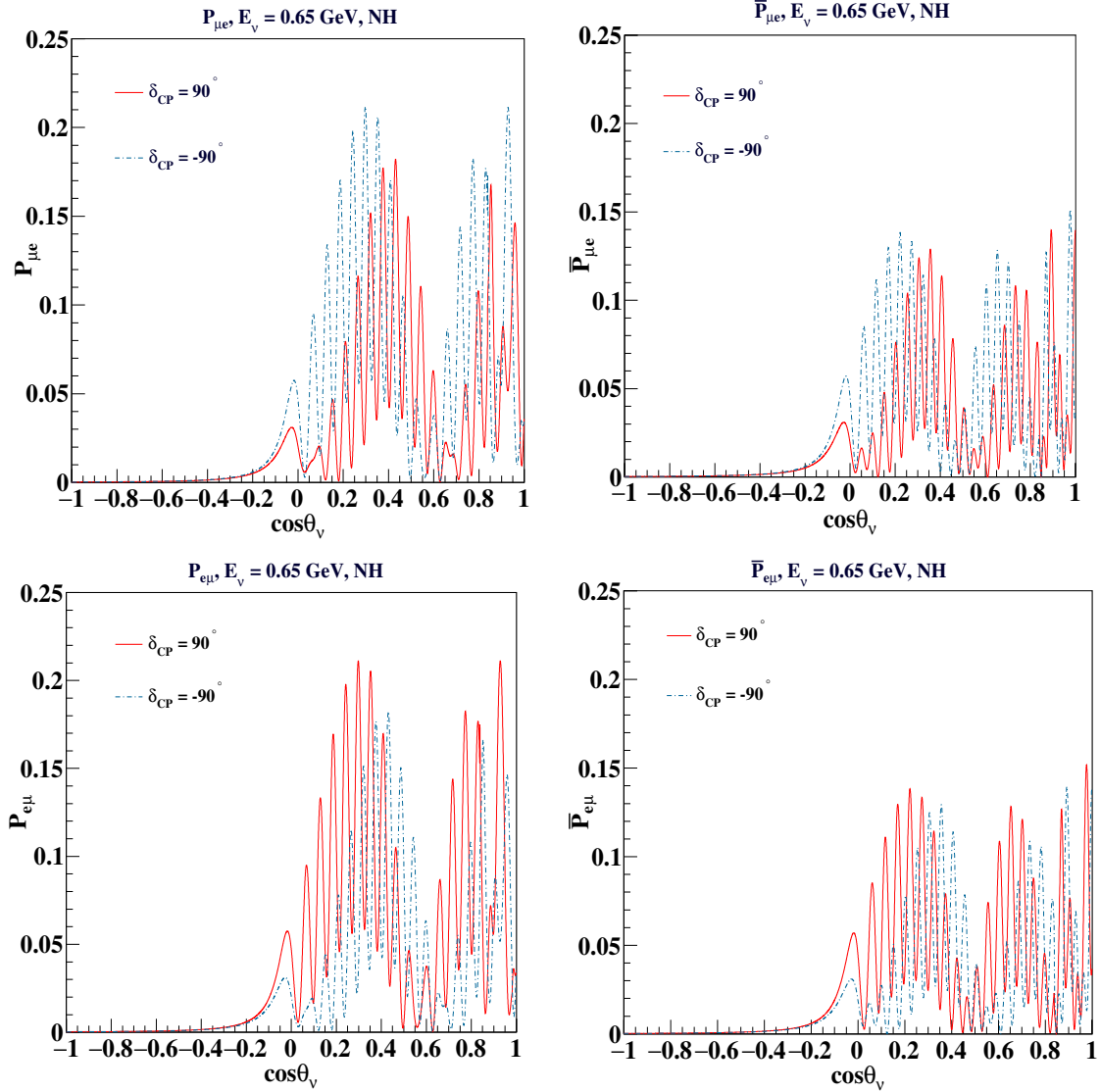


FIG. 1: Transition probabilities  $P_{\mu e}$  (top-left),  $\bar{P}_{\mu e}$  (top-right),  $P_{e\mu}$  (bottom-left) and  $\bar{P}_{e\mu}$  (bottom-right) as a function of  $\cos \theta_\nu$  for a fixed neutrino energy,  $E_\nu = 0.65$  GeV and true normal mass hierarchy.

The probabilities are flipped for  $P_{\mu e}$  ( $\bar{P}_{\mu e}$ ) and  $P_{e\mu}$  ( $\bar{P}_{e\mu}$ ) when  $\delta_{CP}$  changes from  $90^\circ \leftrightarrow -90^\circ$ . In each case, the probabilities with one value of  $\delta_{CP}$ , say  $90^\circ$  is not always below that with  $-90^\circ$ , i.e., the trend is not consistently larger or smaller in all bins, but shows an oscillatory pattern.

A similar behaviour can be seen if we plot the events spectra as a function of  $\cos\theta_\nu$ , as in Fig. 2. The events are generated with parameters given in Table. I. Here the oscillated events are plotted as a function of  $\cos\theta_\nu$  for bins of final state lepton energy and angle,  $E_l = 0.5\text{--}0.8$  GeV and  $\cos\theta_l = 0.6\text{--}0.7$ , where  $l = e, \mu$ . The event spectrum follows the oscillatory behaviour of the transition probabilities plotted in Fig. 1, where some bins have more events when  $\delta_{CP} = +90^\circ$  than  $-90^\circ$ , while it is reversed in other bins. But when we plot the events as a function of the lepton direction  $\cos\theta_l$ , which is the true observable, the behaviour changes as shown in Fig. 3.

It can be seen from Fig. 3 that when the oscillated events are plotted as a function of  $\cos\theta_l$ , the spectrum with  $\delta_{CP} = -90^\circ$  is always greater (less) than that with  $90^\circ$  for  $\nu_e$  and  $\bar{\nu}_e$  ( $\nu_\mu$  and  $\bar{\nu}_\mu$ ), although the effect is smaller for muon neutrinos. That is, the ‘‘oscillatory’’ dependence on  $\delta_{CP}$  seen in Figs. 1 and 2 has disappeared, giving rise to a *systematic dependence* on the CP phase. This effect is due to the kinematics of the interaction which generates a final state lepton scattered at an angle that can be far different from that of the parent neutrino. This is especially so at low energies of interest here, where the dominant process is quasi-elastic (QE) neutrino-nucleus scattering.

Thus, when plotted as a function of  $\cos\theta_l$ , the features of the underlying oscillation probability are lost but the sensitivity to  $\delta_{CP}$  is reinforced. This behaviour, arising because of the different distributions of the final state lepton due to the kinematics of the interaction has not been discussed in the literature before. Again, the same systematic behaviour is also seen in muon events. Although the effect is weaker,  $\delta_{CP}$  dependence is opposite to that of electron events.

The cumulative sum of events as a function of  $\cos\theta_\nu$  is shown in Fig. 4 to illustrate this. It can be seen that though the actual distribution of events in  $\cos\theta_\nu$  follows the oscillation probabilities, scattering of neutrinos coming from several neutrino directions  $\cos\theta_\nu$ , give rise to leptons with the same scattering angle,  $\cos\theta_l$ . For instance, neutrinos with  $\cos\theta_\nu$  practically from  $-1$  to  $+1$  contribute to the events in the bin with  $0.6 \leq \cos\theta_l \leq 0.7$ .

When we sum over these events, their contributions to each  $\cos\theta_l$  bin do not resemble the probabilities, but follow a pattern in which the events spectrum with a particular value of  $\delta_{CP}$  is always greater than the other because of the kinematics of the events. In addition, we have shown all plots so far assuming the normal hierarchy. We will now show, both analytically and numerically, that these results hold, irrespective of the MH.

### III. HIERARCHY (IN)DEPENDENCE AT LOW ENERGIES

In this section we show that at low energies there is no hierarchy ambiguity for atmospheric neutrinos and hence  $\delta_{CP}$  can be measured irrespective of hierarchy. In fact, this can be established analytically as we show here.

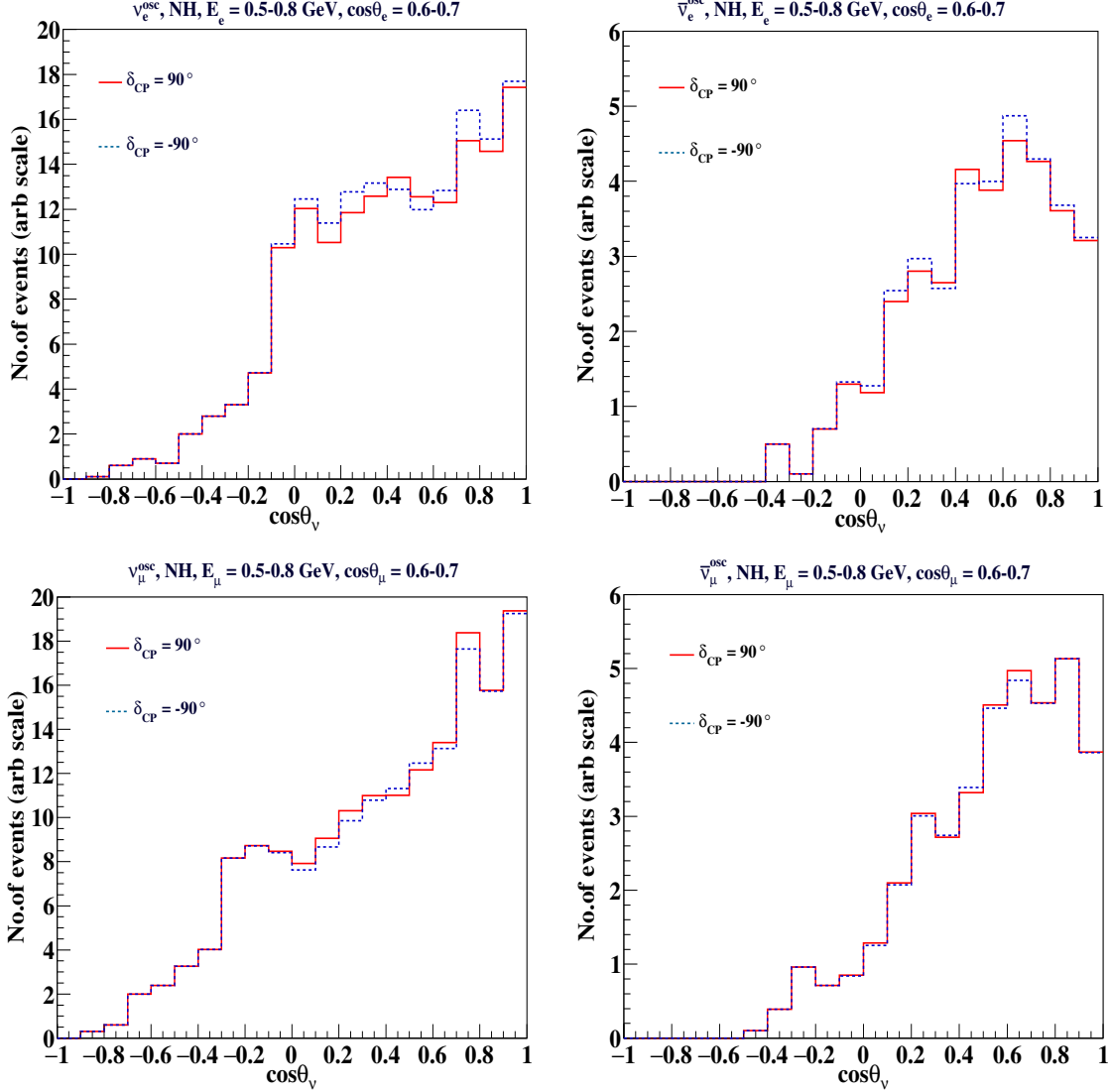


FIG. 2: (Top) Oscillated electron type; (bottom) muon type events as a function of neutrino direction,  $\cos \theta_\nu$ , for events with final lepton energy,  $E_l = 0.5\text{--}0.8$  GeV and direction  $\cos \theta_l = 0.6\text{--}0.7$ , with  $\delta_{CP} = \pm 90^\circ$  and true NH. The left panels are for  $\nu$  events and the right ones are for  $\bar{\nu}$  events.

### A. Hierarchy independence: analytic approach

The 3-flavour vacuum oscillation probability of a flavour  $\nu_\alpha \rightarrow \nu_\beta$  is given by :

$$\begin{aligned}
 P_{\alpha\beta}^{(-)vac} &= \delta_{\alpha\beta} - 4 \sum_{i>j} \text{Re} [U_{\alpha i} U_{\beta i}^* U_{\alpha j}^* U_{\beta j}] \sin^2 \left( \frac{1.27 \Delta m_{ij}^2 L}{E} \right) \\
 &\quad \pm 2 \sum_{i>j} \text{Im} [U_{\alpha i} U_{\beta i}^* U_{\alpha j}^* U_{\beta j}] \sin \left( \frac{2.53 \Delta m_{ij}^2 L}{E} \right),
 \end{aligned} \tag{1}$$

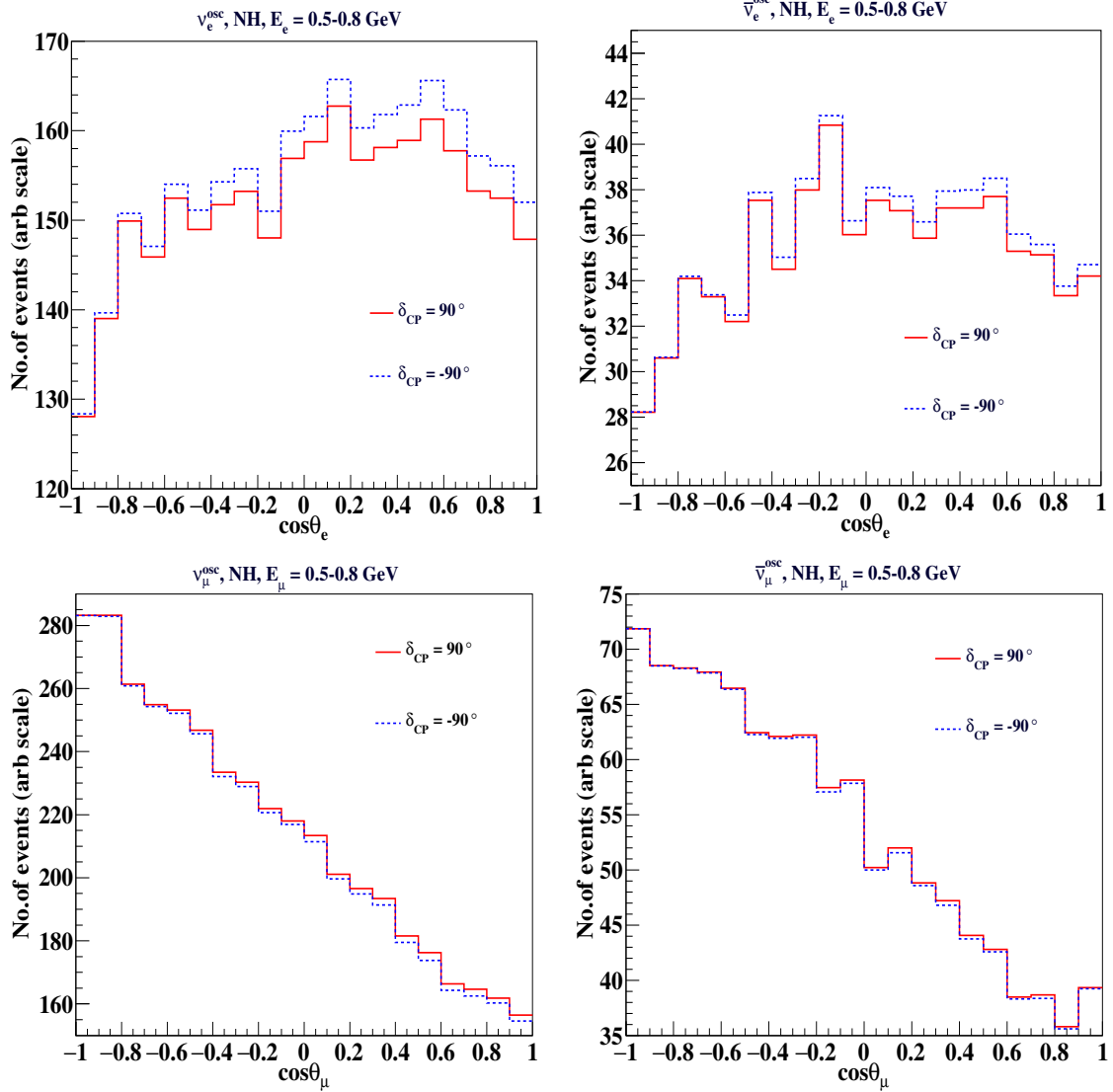


FIG. 3: (Top) Oscillated electron type; (bottom) muon type events as a function of the final state lepton angle,  $\cos\theta_l$ , for events with final lepton energy,  $E_l = 0.5-0.8$  GeV, with  $\delta_{CP} = \pm 90^\circ$  and true NH. The left panels are for  $\nu$  events and the right ones are for  $\bar{\nu}$  events. Note that all y-axes scales are different.

where  $\alpha, \beta = e, \mu, \tau$  are the flavour indices, and the  $\pm$  sign corresponds to neutrinos and anti-neutrinos respectively.

Here

$$U_{\alpha i}^{vac} = \begin{pmatrix} c_{12}c_{13} & s_{12}c_{13} & s_{13}e^{-i\delta} \\ -c_{23}s_{12} - s_{23}c_{12}s_{13}e^{i\delta} & c_{23}c_{12} - s_{23}s_{12}s_{13}e^{i\delta} & s_{23}c_{13} \\ s_{23}s_{12} - c_{23}c_{12}s_{13}e^{i\delta} & -s_{23}c_{12} - c_{23}s_{12}s_{13}e^{i\delta} & c_{23}c_{13} \end{pmatrix},$$

where  $c_{ij} = \cos\theta_{ij}$ ,  $s_{ij} = \sin\theta_{ij}$ ;  $i, j = 1, 2, 3$  are the mass eigenstates,  $\Delta m_{ij}^2 = m_i^2 - m_j^2$  ( $j < i$ ),  $\theta_{ij}$  are the mixing angles and  $\delta_{CP}$  is the leptonic CP violation phase. Here  $L$  (in km) is the distance travelled by a neutrino of energy  $E$  (in GeV).

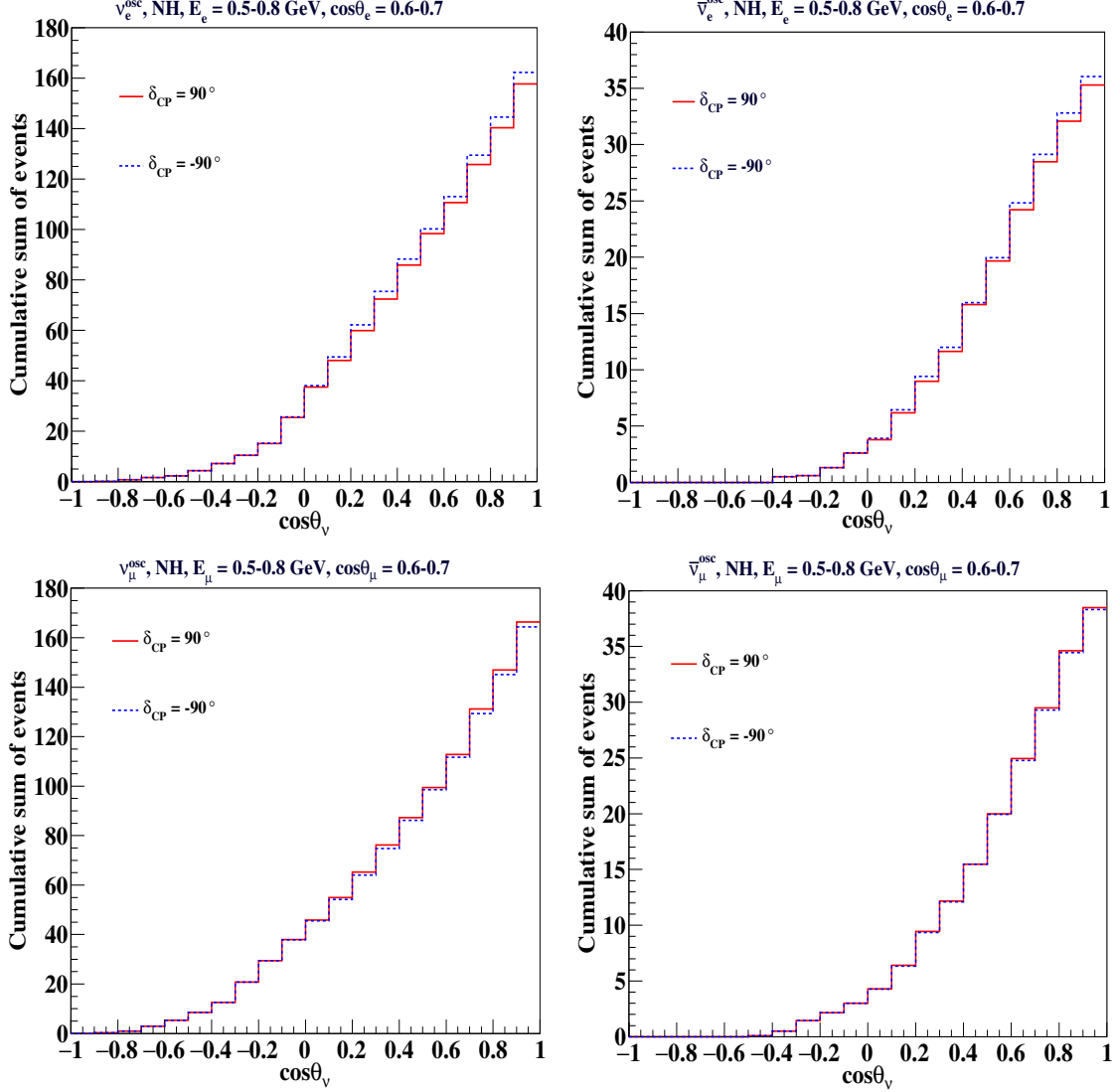


FIG. 4: Cumulative sum of oscillated (top) electron type (bottom) muon type events, which contribute to the  $\cos \theta_l$  bin 0.6–0.7, as a function of  $\cos \theta_\nu$  for the bin  $E_l = 0.5$ –0.8 GeV with  $\delta_{CP} = \pm 90^\circ$  and true NH. The last bin in each plots gives the total contribution to each  $\cos \theta_l$  bin. The left panels are for  $\nu$  events and the right ones are for  $\bar{\nu}$  events.

The survival probability  $P_{\alpha\alpha}$  has no imaginary part, while for transition probabilities  $\alpha \neq \beta$ , the imaginary part changes sign with  $P_{\alpha\beta} = \overline{P}_{\beta\alpha}$ , the corresponding antineutrino probability. When  $E$  is small, of the order of a few hundred MeV, the corresponding oscillatory terms average out whenever  $L/E$  is large compared to  $\Delta m_{ij}^2$ . Since  $|\Delta m_{3j}^2| \sim 2.4 \times 10^{-3} \text{ eV}^2 \gg \Delta m_{21}^2 \sim 7.6 \times 10^{-5} \text{ eV}^2$ ,  $j = 1, 2$ ; this applies to the “atmospheric” terms :

$$1.27 \Delta m_{3j}^2 \frac{L}{E} \approx \pi \frac{(L/100 \text{ km})}{(E/0.1 \text{ GeV})}, \quad (2)$$

rather than to “solar” terms :

$$1.27\Delta m_{21}^2 \frac{L}{E} \approx \pi \frac{(L/3000 \text{ km})}{(E/0.1 \text{ GeV})} . \quad (3)$$

It immediately follows that the atmospheric event rates at these low energies and for  $L \geq$  a few 100 km become independent of  $\Delta m_{32}^2$  and  $\Delta m_{31}^2$  and hence of their ordering. The solar mass-squared difference remains, but its magnitude and sign are well known. Hence the CP phase dependence can be studied with low energy atmospheric neutrinos, independent of the MH. In particular, as has been discussed in the literature earlier (see, for example, Ref. [21, 24]), the probabilities involving  $e$  and  $\mu$  are linear in  $\sin \delta_{CP}$  and  $\cos \delta_{CP}$ . The survival probabilities are independent of  $\sin \delta_{CP}$  which occurs in the imaginary part of the transition probabilities. In fact,  $P_{ee}$  is independent of both  $\sin \delta_{CP}$  and  $\cos \delta_{CP}$  while  $P_{\mu\mu}$  depends on  $\cos \delta_{CP}$  and  $\cos 2\delta_{CP}$ . The transition probabilities  $P_{e\mu}$  and  $P_{\mu e}$  are thus most sensitive to  $\delta_{CP}$ , measurable in principle, via a CP asymmetry, that can be expressed in vacuum as,

$$A_{CP} = \frac{P_{e\mu} - P_{\mu e}}{P_{e\mu} + P_{\mu e}} = -\frac{C}{A + B \cos \delta} \sin \delta \quad (4)$$

$$\bar{A}_{CP} = \frac{\bar{P}_{e\mu} - \bar{P}_{\mu e}}{\bar{P}_{e\mu} + \bar{P}_{\mu e}} = \frac{C}{A + B \cos \delta} \sin \delta \quad (5)$$

for  $\nu$  and  $\bar{\nu}$  respectively. In matter,  $A, B, C$  are modified according to Earth matter effects on the oscillation parameters. The linear dependence on  $\cos \delta_{CP}$  and  $\sin \delta_{CP}$  remains unaltered. See Appendix A for details.

## B. Hierarchy independence: Events spectra at low energies

It is known that Earth matter resonance occurs in atmospheric neutrinos at a few GeV energies thus enabling the determination of the neutrino mass hierarchy. The advantage of using atmospheric neutrinos for hierarchy determination is that it can be determined *unambiguously* of  $\delta_{CP}$ , especially using the  $P_{\mu\mu}$  ( $\bar{P}_{\mu\mu}$ ) survival channel. We have now shown that, at lower energies (sub GeV range) this effect is reversed, i.e.,  $\delta_{CP}$  can be determined irrespective of the hierarchy. In addition, we examined the CP sensitivity of the events as a function of the final lepton scattering angle,  $\cos \theta_l$ . We now show that the systematic dependence on  $\delta_{CP}$  remains when we integrate out the angular dependence and examine the events as a function of the final state lepton energy,  $E_l$  alone.

This is illustrated with oscillated  $\nu_e$  and  $\bar{\nu}_e$  events binned in  $E_l$  in the ranges 0.1–2.0 and 2.0–11.0 GeV in Fig. 5. Here the events are averaged over all directions. Only  $\nu_e$  and  $\bar{\nu}_e$  events are shown in this figure. The effect is similar in  $\nu_\mu$  and  $\bar{\nu}_\mu$  events, but the  $\delta_{CP}$  sensitivity is smaller in  $\nu_\mu$  and  $\bar{\nu}_\mu$  events. It can be seen from the figure that in the lower energy range 0.1–2.0 GeV, the NH and IH spectra with the same true  $\delta_{CP}$  are the same, while the spectra for different true  $\delta_{CP}$  values differ. In the higher energy range from 2.0–11.0 GeV, this effect is reversed. Thus in the lower energy range we can measure  $\delta_{CP}$  irrespective of hierarchy and in the higher energy range hierarchy can be determined irrespective of  $\delta_{CP}$ . This is a unique signature provided only by atmospheric neutrinos: that neutrinos of different energies from the same source can be used to probe different oscillation



parameters unambiguously. The flux of atmospheric neutrinos is smaller than that of the accelerator neutrino experiments; however, the simultaneous availability of a wide range of energies ( $E$ ) and baselines ( $L$ ) and  $\nu$  and  $\bar{\nu}$  and of different neutrino flavours, is a great advantage. In addition to the  $\delta_{CP}$  sensitivity from the accelerator LBL experiments we can add the sensitivities from low atmospheric neutrino experiments thus increasing the global sensitivity towards this parameter.

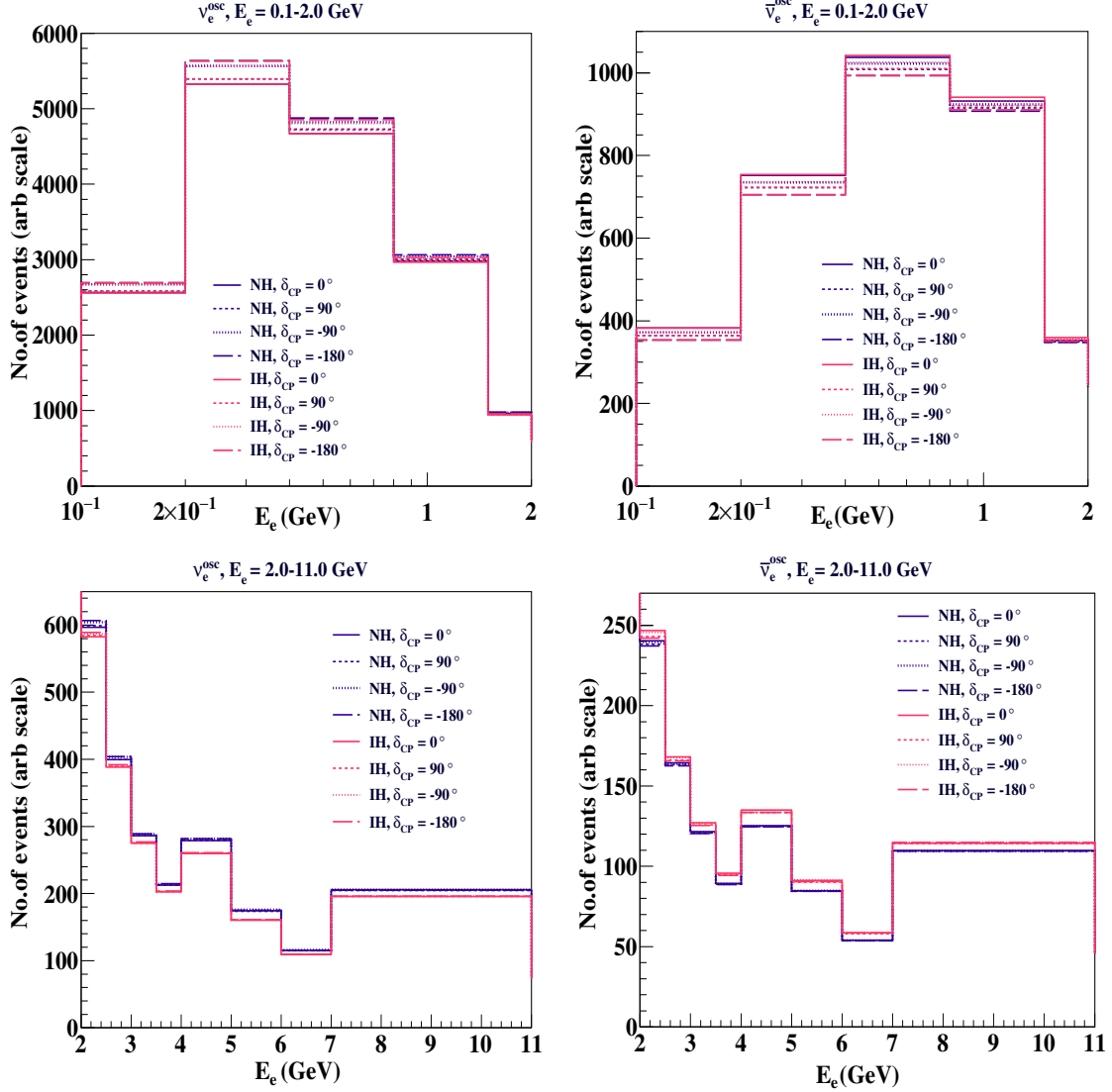


FIG. 5: Oscillated events with different  $\delta_{CP}$  values in the  $E_e$  range (top) 0.1–2.0 GeV and (bottom) 2.0–11.0 GeV. The blue (pink) histograms are for normal (inverted) hierarchy. The left panels are for  $\nu$  events and the right ones are for  $\bar{\nu}$  events. Note that the y-axes are kept different for visibility.

#### IV. SENSITIVITY TO $\delta_{CP}$ WITH LOW ENERGY ATMOSPHERIC NEUTRINOS

It has been shown in the previous sections that at low energies ( $E_\nu < 1$  GeV) the events spectra from different values of  $\delta_{CP}$  can be distinguished from one another *independent* of the neutrino mass hierarchy. This means that a good sensitivity to  $\delta_{CP}$  can be obtained by analyzing low energy atmospheric neutrino events. We now proceed to quantify this sensitivity through a simple  $\chi^2$  analysis. No details of detectors are included; the aim is to establish the  $\delta_{CP}$  dependence *in principle* through an analysis of low energy atmospheric neutrino events.

The events of interest here are those from the charged current (CC) interactions of  $\nu_\mu, \bar{\nu}_\mu, \nu_e$  and  $\bar{\nu}_e$ . The sensitivity to  $\delta_{CP}$  comes mainly from CC  $\nu_e$  and  $\bar{\nu}_e$  events. Since the atmospheric neutrino flux contains both  $\nu_e$  and  $\nu_\mu$  neutrinos and anti-neutrinos, the  $\nu_e$  events detected at the detector can be from the direct  $\nu_e \rightarrow \nu_e$  survived events as well as from the  $\nu_\mu \rightarrow \nu_e$  oscillated events. The number of charged current (CC)  $\nu_e$  events detected is given by :

$$\mathcal{N}^e = t \times n_d \times \int d\sigma_{\nu_e} \times \left[ P_{ee} \frac{d^2\Phi_e}{dE_\nu d\cos\theta_\nu} + P_{\mu e} \frac{d^2\Phi_\mu}{dE_\nu d\cos\theta_\nu} \right], \quad (6)$$

where  $t$  is the exposure time,  $n_d$  is the number of targets in the detector,  $d\sigma_{\nu_e}$  is the differential neutrino interaction cross section (typically differential in  $E_l$ ,  $\cos\theta_l$ , or both), and  $d\Phi_{\nu_\mu}$  and  $d\Phi_{\nu_e}$  are the  $\nu_\mu$  and  $\nu_e$  fluxes. A similar expression holds for muon neutrino and anti-neutrino events as well.

Events are simulated using the NUANCE [25] neutrino generator; here 5000 kton-years of unoscillated events are generated using Honda fluxes and a generic isoscalar target, and scaled down to 500 kton years to reduce fluctuations. “Data” is simulated with the central values of the parameters shown in Table. I and fitted to the “theory” events which are generated by varying the oscillation parameters in their respective  $3\sigma$  ranges.

Parameter	True value	Marginalization range
$\theta_{13}$	$8.5^\circ$	$[7.80^\circ, 9.11^\circ]$
$\sin^2\theta_{23}$	0.5	$[0.39, 0.64]$
$\Delta m_{eff}^2$	$2.4 \times 10^{-3} \text{ eV}^2$	$[2.3, 2.6] \times 10^{-3} \text{ eV}^2$
$\sin^2_{12}$	0.304	Not marginalised
$\Delta m_{21}^2$	$7.6 \times 10^{-5} \text{ eV}^2$	Not marginalised
$\delta_{CP}$	$0, \pm 90^\circ, \pm 180^\circ$	$[-180^\circ, 180^\circ]$

TABLE I: True values and  $3\sigma$  ranges of parameters used to generate oscillated events. Values except that of  $\delta_{CP}$  are taken as in Ref. [26]. For the oscillation analysis,  $\Delta m_{31}^2 = \Delta m_{eff}^2 + \Delta m_{21}^2 (\cos^2\theta_{12} - \cos\delta_{CP} \sin\theta_{13} \sin 2\theta_{12} \tan\theta_{23})$ ;  $\Delta m_{32}^2 = \Delta m_{31}^2 - \Delta m_{21}^2$ , for normal hierarchy when  $\Delta m_{eff}^2 > 0$ . When  $\Delta m_{eff}^2 < 0$ ,  $\Delta m_{31}^2 \leftrightarrow -\Delta m_{32}^2$  for inverted hierarchy.

The event generation and application of oscillations on events are performed as described in [20]. The oscillated events are binned in  $(E_l^{obs}, \cos\theta_l^{obs}, E_{had}^{obs})$ , where  $E_l^{obs}, \cos\theta_l^{obs}$  are the energy and direction of the lepton in the final state,  $l = e, \mu$ ; and  $E_{had}^{obs}$  is the observed final state hadron energy. The bins used for this analysis are shown in Table II. Typical events

Observable	Range	Bin width	No.of bins
$E_l^{obs}$ (GeV) (17 bins)	[0.1, 0.2]	0.1	1
	[0.2, 0.4]	0.2	1
	[0.4, 0.5]	0.1	1
	[0.5, 1.0]	0.3	2
	[1, 4]	0.5	6
	[4, 7]	1	3
	[7, 11]	4	1
	[11, 12.5]	1.5	1
	[12.5, 15]	2.5	1
	[15, 30]	15	1
$\cos \theta_\mu^{obs}$ (20 bins)	[-1.0, 1.0]	0.10	20
$E_{had}^{obs}$ (GeV) (4 bins)	[0, 2]	1	2
	[2, 4]	2	1
	[4, 15]	11	1

TABLE II: The binning scheme used in the analysis. Note that the hadron energy bins are only relevant for the higher energy sample.

spectra as a function of  $\cos \theta_l$  for different values of  $E_l$ , 0.2–0.4 and 0.5–0.8 GeV respectively, are shown in Figs. 6 and 7.

It is clearly evident that the effect of  $\delta_{CP}$  is more in the electron type events than in the muon type events. For a given type of event the separation between the spectra with different  $\delta_{CP}$  is more at lower energies and decreases with the increase of energy. Also at very low energies the difference is consistent for both the up and down directions, whereas at higher energies, the effect is more in the up direction. Because of these consistent differences we can distinguish different  $\delta_{CP}$  values when the events are binned in final state lepton direction.

### A. $\chi^2$ analysis

A Poissonian  $\chi^2$  analysis assuming an isoscalar detector and no systematic uncertainties was performed. This is a hypothetical case to understand how much sensitivity could be obtained under perfect conditions. The perfect detector has 100% reconstruction efficiency for all events and has perfect energy and direction resolutions. In addition to these, it is assumed that there is perfect separation between CC  $\nu_e$ ,  $\bar{\nu}_e$ ,  $\nu_\mu$  and  $\bar{\nu}_\mu$  events. Hence the  $\chi^2$  can be expressed as :

$$\chi_{l\pm}^2 = \sum_i \sum_j \sum_k 2 \left[ (T_{ijk}^{l\pm} - D_{ijk}^{l\pm}) - D_{ijk}^{l\pm} \ln \left( \frac{T_{ijk}^{l\pm}}{D_{ijk}^{l\pm}} \right) \right], \quad (7)$$

where  $i, j, k$  are the indices corresponding to  $E_l, \cos \theta_l, E^{had}$  bins respectively, the last being the total hadronic energy in the final state which is not relevant for the low energy events of interest here. Here  $l = e, \mu$  are the final state leptons;  $T_{ijk}^{l\pm}$  and  $D_{ijk}^{l\pm}$  are the theory

and “data” events respectively; + stands for anti-neutrino events and – for neutrino events. When we can separate neutrinos from anti-neutrinos, the corresponding  $\chi^2$ s can be found out separately as shown here. The total  $\chi_l^2$  for  $l$  type of events is then :

$$\chi_{l\delta_{CP}}^2 = \chi_{l+}^2 + \chi_{l-}^2 . \quad (8)$$

### B. Results - sensitivity to $\delta_{CP}$

The sensitivity to the CP phase has been performed with two different true values  $\delta_{CP}^{true} = 0, -90^\circ$ . Analyses with all parameters fixed as well as parameters other than  $\delta_{CP}$  marginalised in their  $3\sigma$  ranges are also performed. Two different cases are considered, the first in which  $\nu_e, \bar{\nu}_e, \nu_\mu$  and  $\bar{\nu}_\mu$  all can be separately identified. In this case muon charge identification will help in separating  $\nu_\mu$  and  $\bar{\nu}_\mu$ . In the second case there is separation between  $e$  type and  $\mu$  type, but  $\nu_e$  and  $\bar{\nu}_e$  cannot be separated from each other and for muons there is no charge

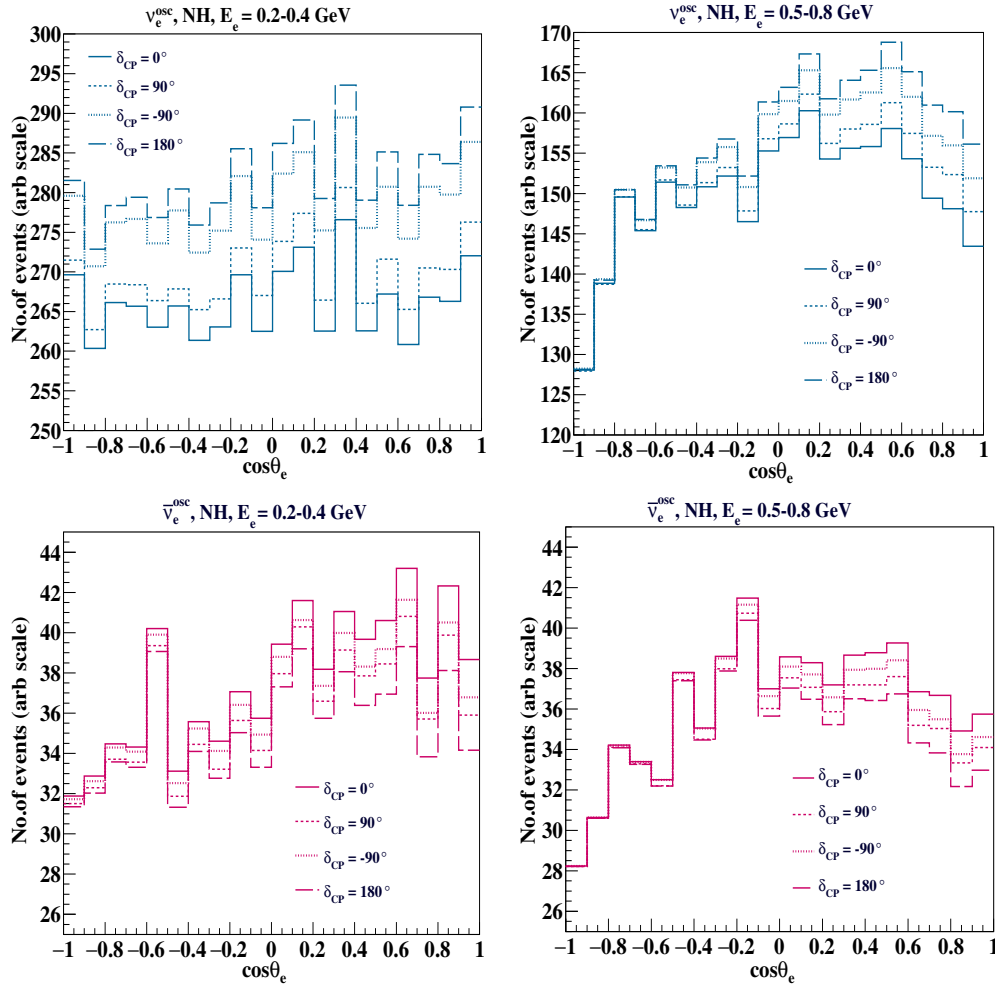


FIG. 6: Electron events for different true  $\delta_{CP}$  values as a function of  $\cos\theta_l^{obs}$  for  $E_l^{obs} = 0.2-0.4$  and  $0.5-0.8$  GeV;  $l = e$ . The top row is for  $\nu$  events and the bottom one for  $\bar{\nu}$ . The y-axes are not the same.

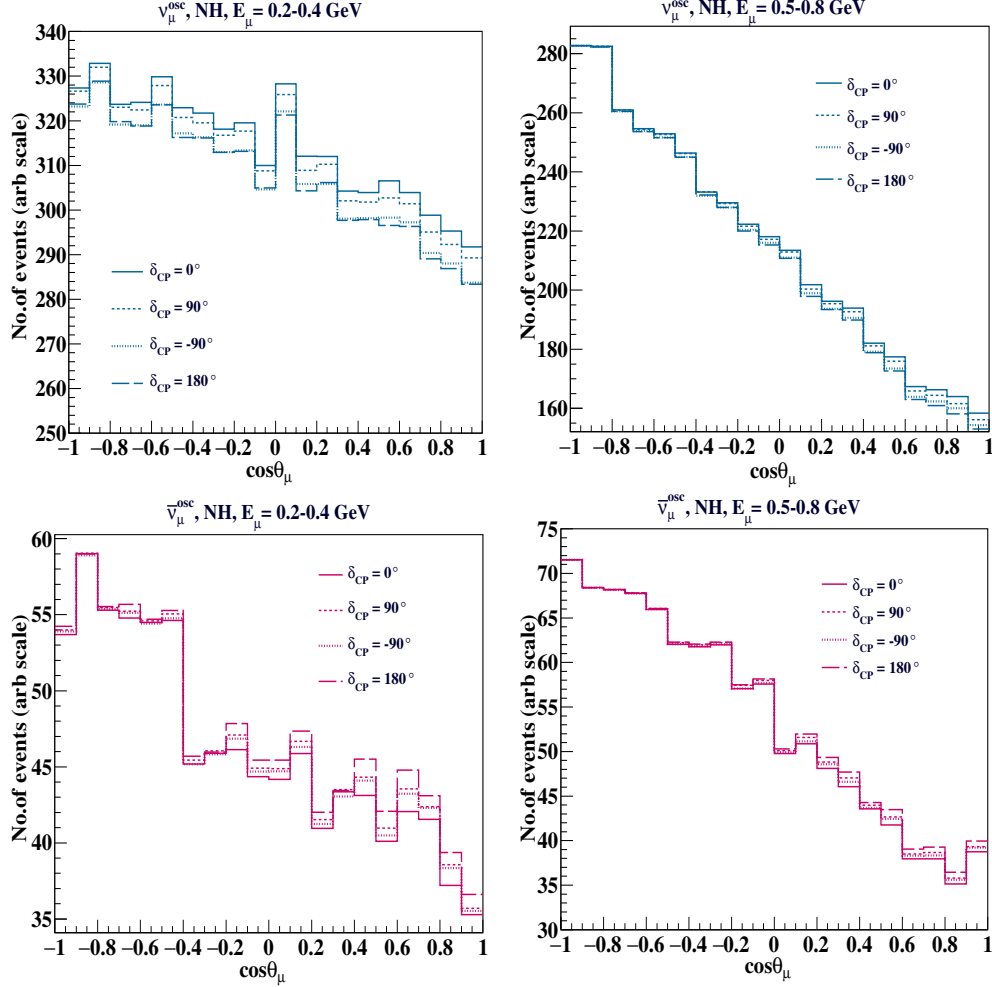


FIG. 7: As in Fig. 6, for muon events,  $l = \mu$ . Again, the  $y$  axes scales are not the same.

identification to separate  $\nu_\mu$  and  $\bar{\nu}_\mu$ . A comparison of the  $\chi^2$  sensitivities are shown in the following figures.

The sensitivity to  $\delta_{CP}$  when  $\nu_e$  ( $\nu_\mu$ ) and  $\bar{\nu}_e$  ( $\bar{\nu}_\mu$ ) can be separated is shown in the left (right) panel of Fig. 8. From the figure it can be readily seen that electron type events have very high sensitivity to  $\delta_{CP}$  as compared to muon type events, which is expected. But at the same time it is appreciable how muon type events can contribute to  $\delta_{CP}$  sensitivity. This is by virtue of adding the low energy neutrino events which are sensitive to  $\delta_{CP}$ . Consider the situation where we have an atmospheric muon neutrino detector only. If this detector can be designed in such a way as to detect neutrinos in energy range  $0.1 - 30.0$  GeV, especially those below 1 GeV and can be magnetised, it can give a very good sensitivity to  $\delta_{CP}$  from muon events alone at low energy, and to the MH at higher energies.

If the true value of  $\delta_{CP}$  is  $-90^\circ$ , then the parameter space except that from  $-135^\circ$  to  $-60^\circ$  can be excluded above  $2\sigma$ . Whereas electron type events can exclude the same region around  $2\sigma$ , the contribution from muon type events is important, since, when combined with that from electron type events, the  $\chi^2$  increases, thus enabling the exclusions better.

The sensitivity to  $\delta_{CP}$  when there is separation between electron type and muon type

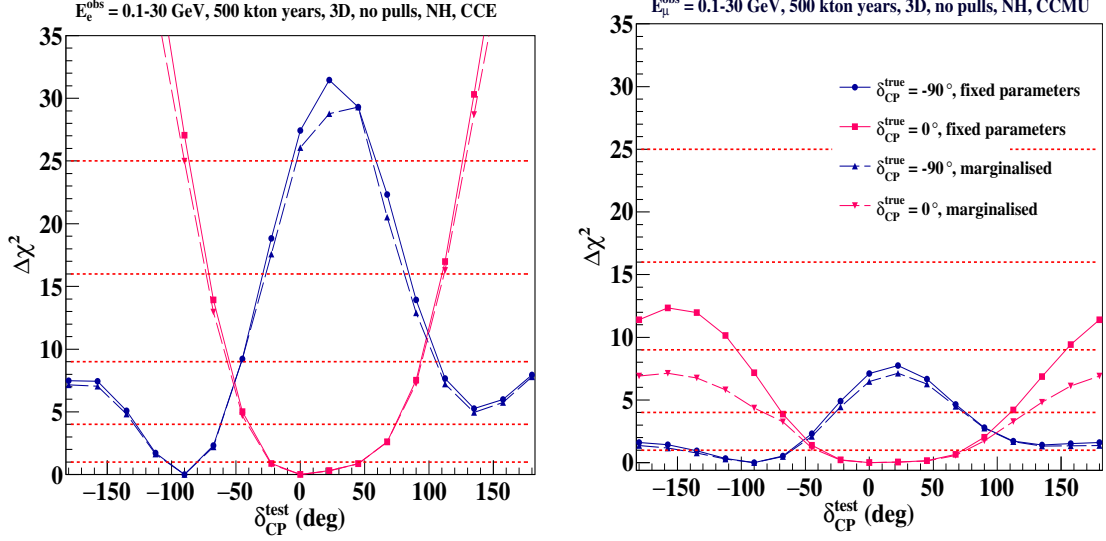


FIG. 8:  $\Delta\chi^2$  vs  $\delta_{CP}^{true}$  (deg) from CC  $\nu_e + \bar{\nu}_e$  (left) and CC  $\nu_\mu + \bar{\nu}_\mu$  (right) events obtained with 500 kton year of an isoscalar detector; and with cid, with fixed parameters (solid curves) and marginalisation (dashed curves). Here  $\delta_{CP}^{true} = 0, -90^\circ$  (deg). Note that the Y-scales are different.

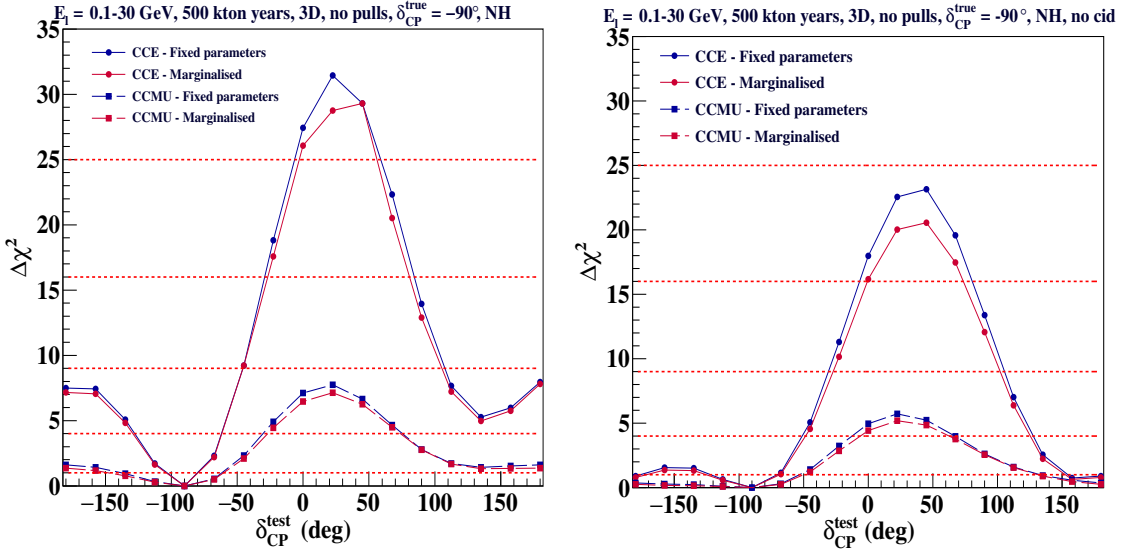
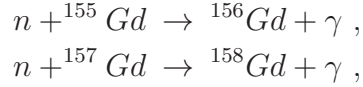


FIG. 9:  $\Delta\chi^2$  vs  $\delta_{CP}^{true}$  (deg) from CC  $\nu_e + \bar{\nu}_e$  (solid) and CC  $\nu_\mu + \bar{\nu}_\mu$  (dot dashed) events obtained with 500 kton year of an isoscalar detector and (left) with cid and (right) no cid. Here  $\delta_{CP}^{true} = -90^\circ$  (deg) is assumed.

events but neutrino events cannot be separated from anti-neutrino events is shown in Fig. 9. Then the sensitivity to  $\delta_{CP}$  is smaller, as compared to the case where  $\nu$  and  $\bar{\nu}$  can be identified separately. This is shown in Fig. 9 where  $\delta_{CP}^{true} = -90^\circ$ . Here it can be seen that the region  $\delta_{CP} \approx [-30^\circ, 80^\circ]$  could be excluded above  $4\sigma$  with  $\nu_e - \bar{\nu}_e$  separation, but it reduces to below  $4\sigma$  when they cannot be. A similar result holds for muon type events.

From Figs. 8 and 9, it can be seen that a detector where we can separate electron type events from muon type events and also neutrinos and anti-neutrinos in both cases will give a better sensitivity to  $\delta_{CP}$ . Of course, this sensitivity will be reduced when realistic detector resolutions and systematic errors are taken into account, but the fact to note is the large discrimination of  $\delta_{CP}$  possible with low energy atmospheric neutrinos, due to the large  $\chi^2$  involved. Also note that bin-to-bin correlations among the data will not affect the results since the sensitivity to  $\delta_{CP}$  is such that the events in all bins are systematically larger or smaller for a given  $\delta_{CP}$ . The separation between  $\nu_\mu$  and  $\bar{\nu}_\mu$  can be easily achieved by having a magnetised detector which will help in identifying the charge of the muon such as with the proposed ICAL detector at INO [8]. Compared to muon type events it is difficult to separate  $\nu_e$  from  $\bar{\nu}_e$ . One of the techniques which can be used to separate  $\nu_e$  and  $\bar{\nu}_e$  is to dope the detector material say water with Gadolinium (Gd) [27–32]. The charged current interaction of  $\bar{\nu}_e$  on a free proton produces a thermal neutron:  $\bar{\nu}_e + p \rightarrow e^+ + n$ , which can be captured on Gd. The reactions :



produce  $\gamma$  rays of energies 8.5 and 7.9 MeV respectively. Then  $\bar{\nu}_e$  can be identified by the coincident detection of  $e^+$  and the  $\gamma$ . This reaction happens only for  $\bar{\nu}_e$  and can be used to separately identify  $\nu_e$  and  $\bar{\nu}_e$ . In addition, the quasi-elastic cross sections for  $\bar{\nu}_e p$  are proportional to  $E_\nu^2$  and are large compared to other processes, especially at low energy, where the cross section is linearly dependent on  $E_\nu$  and so the events sample is large as well. This technique has been proposed for detecting supernova neutrinos [31, 33], but it can be used to detect low energy atmospheric  $\bar{\nu}_e$  also and can be employed in Super-K [5] and Hyper-K [9].

## V. CONCLUSIONS

A study of how low energy atmospheric neutrinos can be used to determine the Dirac CP violating phase  $\delta_{CP}$  in the leptonic sector is performed. It is seen that the events spectra binned according to the final state lepton direction shows consistent distinction between various values of  $\delta_{CP}$ . This allows a precise determination of  $\delta_{CP}$ . Also the major issue of hierarchy ambiguity with  $\delta_{CP}$  vanishes at sub GeV energies enabling a clean measurement of  $\delta_{CP}$ . For a perfect detector a very good  $\chi^2$  is obtained for  $\delta_{CP}$ , the major contribution coming from electron like events. Muon like events also contribute even though in a less sensitive way. But it is very important to analyse all possible events since neutrino experiments are low counting ones and every event adds to the statistics of the experiment. It was also found that when  $\nu_e, \bar{\nu}_e, \nu_\mu$  and  $\bar{\nu}_\mu$  can be separated from one another,  $\delta_{CP}$  sensitivity is higher than the case when  $\nu$  and  $\bar{\nu}$  cannot be separated from each other. This necessitates having special detectors which can distinguish between  $\nu_e$  and  $\bar{\nu}_e$ . Gd doped water Cerenkov detectors are one class of detectors which can achieve this.

Accelerator long baseline experiments like DUNE themselves can determine  $\delta_{CP}$  with very high precision because of the large statistics and the excellent resolutions of the detector. But the sub GeV energy atmospheric neutrinos should not be abandoned since they provide an alternate method of determining  $\delta_{CP}$ , *independent of the neutrino mass hierarchy* and

the results will add to the global sensitivity to  $\delta_{CP}$  thus increasing the overall sensitivity to the parameter. It will be interesting to study how well can different atmospheric neutrino detectors probe  $\delta_{CP}$  especially in the sub GeV range and whether any modification to detector configurations will improve the sensitivity to this parameter. A detailed analysis including detector resolutions and systematic effects is beyond the scope of this paper and is work in progress.

## VI. ACKNOWLEDGEMENTS

We are grateful to Prof.G. Rajasekaran and Prof. Rahul Sinha, IMSc Chennai for many discussions. We also thank the Journal Club at IMSc where this idea was first discussed, and Prof.T. Kajita for helpful comments during the EILH workshop at Aligarh Muslim University. LSM thanks Prof. Jim Libby, IIT Madras, Chennai. She also acknowledges Nandadevi cluster which is a part of the computing facility at IMSc Chennai, with which the simulations were performed.

### Appendix A: Details of hierarchy independence at low energies

The transition probability in vacuum can be expressed as :

$$P_{\alpha\beta}^{vac} = -4Re[U_{\alpha 2}U_{\beta 2}^*U_{\alpha 1}^*U_{\beta 1}] \sin^2(1.27\Delta m_{21}^2 L/E) \quad (A1)$$

$$-2Re[U_{\alpha 3}U_{\beta 3}^*(\delta_{\alpha\beta} - U_{\alpha 3}^*U_{\beta 3})] \quad (A2)$$

$$+2Im[U_{\alpha 2}U_{\beta 2}^*U_{\alpha 1}^*U_{\beta 1}] \sin(2.53\Delta m_{21}^2 L/E). \quad (A3)$$

Since the probability is independent of  $\Delta m_{32}^2$ , there is no hierarchy ambiguity.

$$P_{e\mu} = A + B \cos \delta - C \sin \delta = \overline{P}_{\mu e};$$

$$P_{\mu e} = A + B \cos \delta + C \sin \delta = \overline{P}_{e\mu},$$

where

$$\begin{aligned} A &= c_{13}^2 \sin^2(2\theta_{12})(c_{23}^2 - (s_{23}s_{13})^2) \sin^2(\delta_{21}/2) + \frac{1}{2}s_{23}^2 \sin^2(2\theta_{13}), \\ B &= (1/4)c_{13} \sin(4\theta_{12}) \sin(2\theta_{13}) \sin(2\theta_{23}) \sin^2(\delta_{21}/2), \\ C &= (1/4)c_{13} \sin(2\theta_{12}) \sin(2\theta_{13}) \sin(2\theta_{23}) \sin(\delta_{21}), \\ \delta_{21} &= 2.534\Delta m_{21}^2 L/E. \end{aligned}$$

$A, B, C$  are only limited only by precisions measurements of oscillation parameters. The CP asymmetry can be expressed as :

$$A_{CP} = \frac{P_{e\mu} - P_{\mu e}}{P_{e\mu} + P_{\mu e}} = -\frac{C}{A + B \cos \delta} \sin \delta \quad (A4)$$

$$\overline{A}_{CP} = \frac{\overline{P}_{e\mu} - \overline{P}_{\mu e}}{\overline{P}_{e\mu} + \overline{P}_{\mu e}} = \frac{C}{A + B \cos \delta} \sin \delta \quad (A5)$$



for  $\nu$  and  $\bar{\nu}$  respectively.

- 
- [1] I. Esteban *et al.*, *Global analysis of three-flavour neutrino oscillations: synergies and tensions in the determination of  $\theta_{23}$ ,  $\delta_{CP}$ , and the mass ordering*, JHEP **01** (2019) 106.
  - [2] K. Abe *et al.* (T2K Collaboration), *Search for CP violation in neutrino and anti-neutrino oscillations by the T2K experiment with  $2.2 \times 10^{21}$  protons on target*, Phys. Rev. Lett. **121**, (2018) 171802.
  - [3] M. A. Acero *et al.* (NOvA Collaboration), *New constraints on oscillation parameters from  $\nu_e$  appearance and  $\nu_\mu$  disappearance in the NOvA experiment*, Phys. Rev. D **98**, (2018) 032012.
  - [4] B. Abiet *et al.*, *The DUNE far detector interim design report Volume 1: Physics, technology and strategies*, arXiv:1807.10334 (2018).
  - [5] M. Jiang, K. Abe *et al.*, (Super-Kamiokande Collaboration), *Atmospheric neutrino oscillation analysis with improved event reconstruction in Super-Kamiokande IV*, arXiv:1901.03230 [hep-ex] (2019).
  - [6] K. Abe *et al.*, *Atmospheric neutrino oscillation analysis with external constraints in Super-Kamiokande I-IV*, Phys. Rev. D **97**, 072001 (2018).
  - [7] Y. Fukuda *et al.*, (Super-Kamiokande Collaboration), *Evidence for oscillation of atmospheric neutrinos*, Phys. Rev. Lett. **81** 1562 (1998).
  - [8] A. Kumar, A. M. Vinod Kumar *et al.*, *Invited review: Physics potential of the ICAL detector at the India-based Neutrino Observatory (INO)*, Pramana J Phys **88** (2017) 79.
  - [9] K. Abe *et al.*, *Letter of intent: The Hyper-Kamiokande experiment – Detector design and physics potential*, arXiv:1109.3262v1 [hep-ex] (2011).
  - [10] K. Abe *et al.*, *Hyper-Kamiokande design report*, KEK preprint (2016).
  - [11] S Adrin-Martinez *et al.*, *Letter of intent for KM3NeT 2.0*, J. Phys. G: Nucl. Part. Phys. **43** 084001 (2016).
  - [12] KM3NeT Collaboration, *Technical design report - Part 1*, (ISBN 978-90-6488-033-9) (2010).
  - [13] M. G. Aartsen *et al.* (The IceCube Gen2 Collaboration), *Letter of intent: The precision IceCube next generation upgrade (PINGU)*, arXiv:1401.2046-v2 [physics.ins-det] (2017).
  - [14] Honda, M. *et al.*, *Calculation of atmospheric neutrino flux using the interaction model calibrated with atmospheric muon data*, Phys. Rev. D **75** (2007) 043006.
  - [15] Honda, M. *et al.*, *Improvement of low energy atmospheric neutrino flux calculation using the JAM nuclear interaction model*, Phys. Rev. D **83** (2011) 123001.
  - [16] Honda, M. *et al.*, *Atmospheric neutrino flux calculation using the NRLMSISE-00 atmospheric model*, Phys. Rev. D **92** (2015) 023004.
  - [17] T. Thakore *et al.*, *The Reach of INO for Atmospheric Neutrino Oscillation Parameters*, JHEP **5** (2013) 058.
  - [18] A. Ghosh *et al.*, *Determining the neutrino mass hierarchy with INO, T2K, NOvA and reactor experiments*, JHEP **4** (2013) 009.
  - [19] M. M. Devi *et al.*, *Enhancing sensitivity to neutrino parameters at INO combining muon and hadron information*, JHEP **10** (2014) 189.
  - [20] Lakshmi. S. Mohan and D. Indumathi, *Pinning down neutrino oscillation parameters in the 2–3 sector with a magnetised atmospheric neutrino detector: a new study*, Eur. Phys. J. C (2017) **77**:54.

- [21] K. Kimura *et al.*, *Exact formula of probability and CP violation for neutrino oscillations in matter*, Phys. Lett. B **537** (2002), 86–94.
- [22] M. Honda *et al.*, *A simple parameterization of matter effects on neutrino oscillations*, arXiv:hep-ph/0602115 (2006).
- [23] P. I. Krastev and S. T. Petcov, *Resonance amplification and T-violation effects in three-neutrino oscillations in the Earth*, Phys. Lett. B **205** (1988) 84–92.
- [24] K. Kimura *et al.*, *Exact formulas and simple CP dependence of neutrino oscillation probabilities in matter with constant density*, Phys. Rev. D **66**, 073005 (2002).
- [25] D. Casper, *The nuance neutrino physics simulation, and the future*, Phys. Proc. Suppl. **112** (2002) 161-170.
- [26] S. Choubey *et al.*, *Sensitivity to neutrino decay with atmospheric neutrinos at the INO-ICAL detector*, Phys. Rev. D **97**, 033005 (2018).
- [27] Takaaki Mori, *Status of the Super-Kamiokande gadolinium project*, NIM A **732** (2013) 316–319.
- [28] Luis Labarga, *The SuperK-gadolinium project*, PoS (HQL 2016) 007.
- [29] John F. Beacom and Mark R. Vagins, *Antineutrino Spectroscopy with Large Water Cherenkov Detectors*, Phys. Rev. Lett. **93**, 171101 (2004).
- [30] P. Fernandez, *Status of GADZOOKS!: Neutron Tagging in Super-Kamiokande* Nuclear and Particle Physics Proceedings 273275 (2016) 353360.
- [31] Takaaki Mori, *Development of a gadolinium-doped water cherenkov detector for the observation of supernova relic neutrinos*, PhD Thesis, The University of Okayama (2015).
- [32] Chenyuan Xu, *Study of a 200 ton gadolinium-loaded water cherenkov detector for Super-KamiokaNDE gadolinium project*, Master Thesis, Okayama University (2016).
- [33] Guillaume Pronost, *Looking for Gd neutron captures from SN  $\nu$  with EGADS detector*, PoS (ICRC2017) 964.